IEEE Access
Multidisciplinary | Rapid Review | Open Access Journal

Received April 17, 2020, accepted April 28, 2020, date of publication May 4, 2020, date of current version May 18, 2020.

Digital Object Identifier 10.1109/ACCESS.2020.2992089

Reliability Assessment of Wind Power Converter Considering SCADA Multistate Parameters Prediction Using FP-Growth, WPT, K-Means and LSTM Network

JINGXUAN ZHANG[1,2], (Student Member, IEEE), HEXU SUN[1,3], (Senior Member, IEEE), ZEXIAN SUN[2], WEICHAO DONG[1,3], YAN DONG[1], (Member, IEEE), AND SIYUAN GONG[4]

[1]School of Artificial Intelligence, Hebei University of Technology, Tianjin 300130, China
[2]College of Electrical Engineering, North China University of Science and Technology, Tangshan 063210, China
[3]School of Electrical Engineering, Hebei University of Science and Technology, Shijiazhuang 050018, China
[4]Department of Science and Information Technology, Hebei Construction and Investment Group Company, Ltd., Shijiazhuang 050000, China

Corresponding author: Hexu Sun (hxsun@hebust.edu.cn)

This work was supported in part by the Key Project of Hebei Natural Fund under Grant E2018210044, in part by the Hebei Education Department Fund under Grant QN2016079, and in part by the Hebei Food and Drug Administration under Grant ZD2015016.

ABSTRACT In order to cooperate the wind farm operators with grasping the operation status of wind power converter, a novel reliability assessment strategy is proposed based on supervisory control and data acquisition (SCADA) multistate parameters prediction of permanent magnet synchronous generator (PMSG) wind turbine. The strategy considers ''off-line training, on-line matching and assessment''. The operation reliability of wind power converter is obtained via the analysis and weight computing of confidence level, prediction value and actual value of SCADA multistate parameters. In the ''off-line training'' part, first, the FP-Growth association algorithm is employed to analyze the confidence levels of SCADA variables to the faults of wind power converter. The variables with high confidence level are defined as SCADA multistate parameters. Afterwards, wavelet packet transform (WPT) and K-means algorithm are employed to decompose, reconstruct, normalize and cluster the time series (off-line data) of multistate parameters under normal operation of wind turbine, to improve the generalization capability of long short term memory (LSTM) prediction model. In the part of ''on-line matching and assessment'', the actual value time series (on-line data) of multistate parameters are decomposed and reconstructed by WPT. Each normalized sample is matched to the closest cluster centroid, which is generated in the part of ''off-line training''. Then the corresponding LSTM model is conducted to predict based on the each sample. The final prediction value is sum of prediction results of entire samples in clusters. Finally, the reliability of wind power converter is assessed by the proposed strategy. The effectiveness of proposed assessment strategy is verified by the experimental results on a PMSG wind power converter.

INDEX TERMS Reliability assessment, wind power converter, association rules algorithm, deep learning, recurrent neural network.

I. INTRODUCTION

Power converter is a crucial device of wind energy conversion system (WECS) in a wind turbine [1]–[3].It is utilized to control the speed and torque of the generator, simultaneously, apply the active and reactive power to the grid in the modern wind turbine system [4]. Over the past decade, a number of investigations and surveys have revealed that as the one of core devices of a wind turbine, the power converter is with the high failure rate, the long downtime, and the low reliability [5]. These have not only greatly increased the production cost of wind power operators, but also seriously impact the stability of grid and even threaten personal safety [6], [7]. Timely and accurate reliability assessment of wind power

The associate editor coordinating the review of this manuscript and approving it for publication was Ton Do.

converter can remind the operators of necessary maintenance and repair of the power converter, so as to effectively reduce the production cost and provide technical support for improving the reliability of wind power converter [8].

A number of studies have been made concerning reliability assessment of wind power converter [9]–[12]. The main research strategies maybe roughly divided into the following two categories: First, compute the lifetime of one of core devices of power converter to assess the reliability. Second, analyze and compute several variables parameter of WECS to assess the reliability. The former needs to know partial electrical parameters of WECS and few environment parameters. By establishing the thermal cycle model of power converter and according to the known reliability coefficients of electronic components, the lifetime of the power converter can roughly be estimated. The latter needs to collect the data of SCADA variables during the normal and failure operation of the power converter for a long time, from which the variables and data characteristics that can reveal whether the power converter is in the failure state are mined, and then the operation status of the power converter is quantitatively analyzed.

As stated in [13], the lifespans of the wind power converter with low and medium speed PMSG are estimated and compared from the thermal cycling of the IGBT module component. However, the obtained reliability metrics of only machine-side converter are rough ranges under extremely severe restrictions, which lead to weak generalization and comparison capability. Health condition of base-plate solder for IGBT module in wind power converter is assessed by analyzing the case temperature difference in [14], but the effects of ambient temperature on heat transfer efficiency of cooling water and on the case temperature are not taken into account, which give other thermal transference of the case of IGBT module. Moreover, as stated in [15], a method to monitor the health of aluminum electrolytic capacitors for enhance the reliability of the modular multilevel converters is introduced.

With the continuous progress and development of science and technology, the wind turbine is developing towards the direction of large-scale, complexity and cost reduction. More and more sensors are utilized in the wind turbine, which makes the variable parameters reflecting the status of each component of the wind turbine more abundant in the SCADA system, thus providing the possibility to assess the reliability of the power converter more comprehensively and accurately. As stated in [16], the health status of wind turbine is assessed by using recurrent neural networks, which is based on the SCADA data of subsystems, but the only a small number of SCADA variables are focused on, and the association levels with the failures of wind turbine are unclear. In this paper, SCADA variables with higher faults confidence levels are selected as multistate parameters to assess the reliability of wind power converter.

The rest of this paper is organized as follows. Section II presents an overview of proposed strategy. Section III reviews the FP-Growth, WPT (including coefficient series normalization), K-means and LSTM algorithm. Afterwards, reliability assessment model of power converter is proposed. Section IV presents results, and discusses the performance with respect to the several methods considered in the investigation. Finally, Section V summarizes the results and conclusions of this study.

II. THE PROPOSED STRATEGY

Until now, the doubly fed induction generator (DFIG) and PMSG wind turbines have occupied the majority of the global wind power market [17], [18]. Initially, the DFIG equipped with partial scale converter became attractive due to the controllability of active and reactive power. However, with the development of technology, the PMSG equipped with full scale converter has more obvious advantages in low-voltage ride-through capability, higher efficiency and power density [19], which is the main development trend of the wind turbine market in the future. Fig. 1 presents the topological graph of the core devices of a PMSG wind turbine system, which includes blade, gear box, PMSG, full scale power converter, filter and transformer. The electric energy converted from wind energy is finally fed to the grid. In this paper, the reliability of power converter of PMSG wind turbine is assessed. The main contributions of this paper are as follows:

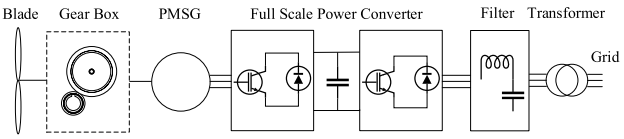

FIGURE 1. The topological graph of the core devices of a PMSG wind turbine.

1) FP-Growth algorithm is utilized to extract the high confidence level variables of wind turbine SCADA as the multistate parameters.

2) The prediction model of each state parameter based on WPT, K-means algorithm and LSTM network is established under normal operation of wind turbine.

3) Conduct WPT for the ''on-line'' time series of SCADA multistate parameters when wind turbine is operating. Make the normalized coefficient series samples match to the closest cluster centroids, which are generated in the ''off-line training'' part. Then the corresponding LSTM model is conducted to predict based on the samples. The final prediction value is sum of prediction results of entire samples in clusters.

4) The reliability of wind power converter is assessed by proposed strategy, which is via the analysis and weight computing of confidence level, prediction value and actual value of SCADA multistate parameters.

III. THE PROPOSED RELIABILITY ASSESSMENT MODEL

A. FP-GROWTH ASSOCIATION RULE ALGORITHM

To distinguish and mine the variables of high confidence level with power converter faults from numerous wind turbine

SCADA variables, FP-Growth association rule algorithm is employed in this paper.

1) FP-GROWTH ALGORITHM

Jiawei Han proposed the FP-Growth algorithm with discovering frequent itemsets using frequent pattern tree (FP-Tree) in 2000 [20]. The FP-Growth method indexes the database for fast computing via FP-Tree. The FP-Tree is constructed as follows. Initially the tree contains as root the null item $\emptyset$. Afterwards, each tuple $\langle t, X\rangle \in D$, where $X = i(t)$ denotes itemset, D denotes database, insert X into FP-Tree, incrementing the count of all nodes along the path that represents X. If X shares a prefix with some previously inserted transaction, then X will follow the same path until the common prefix. For the remaining items in X, new nodes are create under the common prefix, with counts initialized to 1. The FP-Tree is complete when entire transactions have been inserted. At this point, the FP-Tree serves as an index in lieu of the original database. All frequent itemsets can be mined from the tree directly via the FP-Growth method, whose pseudo code is shown in Algorithm 1.

Algorithm 1 FP-Growth Algorithm

// Initialization: $R \leftarrow$ FP-Tree(**D**), $P \leftarrow \emptyset$, $F \leftarrow \emptyset$
FP-Growth(R, P, F, *minsup*):
1 remove infrequent items from R
2 **if** IsPath(R) then // insert subsets of R into F
3 **foreach** $Y \subseteq R$ **do**
4 $X \leftarrow P \cup Y$
5 $sup(X) \leftarrow \min_{x\in Y}\{cnt(x)\}$
6 $F \leftarrow F \cup [1]$
7 **else** //process projected FP-Trees for each frequent item i
8 **foreach** $i \in R$ in increasing order of $sup(i)$ **do**
9 $X \leftarrow P \cup [1]$
10 $sup(X) \leftarrow sup(i)$ //sum of $cnt(i)$ for all nodes labeled i
11 $F \leftarrow F \cup \{(X, sup(X))\}$
12 $R_X \leftarrow \emptyset$ //projected FP-Tree for X
13 **foreach** *path* $\in$ PathFromRoot(i) **do**
14 $cnt(i) \leftarrow$ count of i in *path*
15 inset *path*, excluding i, into FP-Tree R_X with count $cnt(i)$
16 **if** $R_X \neq \emptyset$ **then** FP-Growth(R_X, X, F, *minsup*)

2) GENERATING ASSOCIATION RULES

Given a collection of frequent itemsets F, when a frequent itemset $Z \in F$, look at all proper subsets $X \subset Z$ to compute rules of the form:

$$X \xrightarrow{s,c} Y, Y = \frac{Z}{X} = Z - X \tag{1}$$

The rule must be frequent since:

$$s = sup(XY) = sup(Z) \geq minsup \tag{2}$$

Thus, only checking whether the rule confidence level satisfies the minconf threshold. Confidence is computed as follows:

$$c = \frac{sup(X \cup Y)}{sup(X)} = \frac{sup(Z)}{sup(X)} \tag{3}$$

If $c \geq minconf$, then the rule is a strong rule. Otherwise, if $conf(X \rightarrow Y) < c$, then $conf(W \rightarrow \frac{Z}{W}) < c$ for entire subsets $W \subset X$, since $sup(W) \geq sup(X)$.

B. WAVELET PACKET TRANSFORM AND COEFFICIENT SERIES NORMALIZE

1) WAVELET PACKET TRANSFORM

Wavelet packets are a generalization of orthonormal and compactly supported wavelets [21]. Pioneered by Coifman, Meyer and Wickerhauser, methods of wavelet packet transform have been successfully used for data compression. Wavelet only decomposes low-frequency part of a signal. Compared with wavelet decomposition, both low-frequency and high-frequency parts of a signal are decomposed by wavelet packet. The corresponding frequency band is adaptively selected to match the signal spectrum, thus improving the time-frequency resolution. Fig. 2 presents the mission profile of signal S based 3-level wavelet packet decomposition.

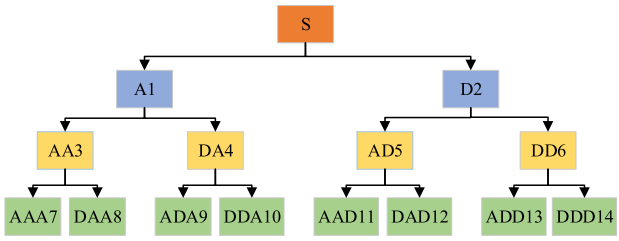

FIGURE 2. The mission profile of signal S based 3-level wavelet packet decomposition.

Where A denotes the low-frequency part of the signal decomposed from the previous level; D denotes the high-frequency part of the signal decomposed from the previous level; Numbers 1-14 denote the node codes of coefficient series.

Scaling function $\varphi(x)$ and wavelet function $\psi(x)$ content two-scale equation:

$$\varphi(x) = \mu_0(x) = \sum_{k\in Z} h(k)\mu_0(2x-k) \tag{4}$$

$$\psi(x) = \mu_1(x) = \sum_{k\in Z} g(k)\mu_0(2x-k) \tag{5}$$

$$\mu_{2p}(x) = \sum_{k\in Z} h(k)\mu_p(2x-k) \tag{6}$$

$$\mu_{2p+1}(x) = \sum_{k\in Z} g(k)\mu_p(2x-k) \tag{7}$$

where $\mu_n(x)(n = 2p \text{ or } n = 2p+1, p = 0, 1, 2, \ldots)$ in (6) and (7) is defined as wavelet packet of orthonormal

scaling function. Equations (6) and (7) could be rewritten as follows:

$$C_{2p}(n) = \sqrt{2}\sum_{k\in Z} h(k)C_p(2n-k) \tag{8}$$

$$C_{2p+1}(n) = \sqrt{2}\sum_{k\in Z} g(k)C_p(2n-k) \tag{9}$$

Thus, (8) and (9) are the wavelet packet decomposition of signals. Two coefficient series are obtained after each wavelet packet decomposition, and these two coefficient series are decomposed in the next level respectively, that is, the decomposition process should be carried out for the low-frequency part and the high-frequency part, so that the resolution of each part of the signal frequency band can be improved.

Mallat algorithm could be employed to reconstruct the coefficient series after wavelet packet decomposition:

$$C_{j+1}(n) = \sum_{k\in Z} h(k-2n)C_j(k) \tag{10}$$

$$d_{j+1}(n) = \sum_{k\in Z} g(k-2n)C_j(k) \tag{11}$$

Let $H = h(k-2n)$, $G = g(k-2n)$, and (10) and (11) could be rewritten as follows:

$$C_{j+1}(n) = HC_j(k) \tag{12}$$

$$d_{j+1}(n) = GC_j(k) \tag{13}$$

Then:

$$C_j(k) = H^*C_{j+1} + G^*d_{j+1} \tag{14}$$

Equation (14) is the reconstruction algorithm of wavelet packet, where H^* and G^* are the dual operators of H and G, respectively. The coefficient series decomposed by wavelet packet could be reconstructed to original signal.

2) COEFFICIENT SERIES NORMALIZE

If the signal time series of length n is decomposed and reconstructed to K levels by wavelet packet, there are 2^K node coefficient series C_k, whose length is n in the K-th level, $k = 1, 2, \ldots, 2^K$. Each node coefficient series is normalized to be the sample coefficient series matrix X_k. If the length of each sample is m, there are $n - m + 1$ samples in X_k.

$$X_k = \begin{bmatrix} X_{k\_1} \\ X_{k\_2} \\ \cdots \\ X_{k\_n-m+1} \end{bmatrix} = \begin{bmatrix} C_k(1) & C_k(2) & \ldots & C_k(m) \\ C_k(2) & C_k(3) & \ldots & C_k(m+1) \\ \cdots & \cdots & \cdots & \cdots \\ C_k(n-m+1) & C_k(n-m+2) & \ldots & C_k(n) \end{bmatrix}, \quad k = 1, 2, \ldots, 2^K \tag{15}$$

where, for instance, X_{k_1} denotes the first sample, which is composed of m coefficients $\begin{bmatrix} C_k(1) & C_k(2) & \ldots & C_k(m) \end{bmatrix}$.

C. K-MEANS ALGORITHM

K-means is a kind of clustering algorithms, which is also an unsupervised learning based on data similarity division. It points the more similar samples into the same cluster. Usually, a distance function $d(X, Y)$ is defined to denote the similarity between samples X and Y. Minkowski distance, Manhattan distance or Euclidean distance is employed. In this paper, Euclidean distance is chosen as the distance function. The two samples are the more similar, the distance is the much less.

Suppose that there are two sample points P and Q, the corresponding coordinates are:

$$P = (x_1, x_2, \ldots, x_n) \in \mathbb{R}^n \tag{16}$$

$$Q = (y_1, y_2, \ldots, y_n) \in \mathbb{R}^n \tag{17}$$

Then, the Euclidean distance between P and Q is expressed:

$$d(P, Q) = \sqrt{\sum_{i=1}^{n}(x_i - y_i)^2} \tag{18}$$

K-means defines a constant k first, where k is the number of clusters. Afterwards, normalizing the cluster centroids. The samples are pointed into the most similar clusters by computing the similarity between each sample and cluster centroid. The steps of K-means algorithm could be expressed as follows:

1) Initialize constant k, and k cluster centroids.
2) Iterate the following process until the cluster centroids would not change.
   i) Compute the similarity between each sample and cluster centroid. Divide the samples into the most similar clusters.
   ii) Compute the mean of samples divided into each cluster. The mean is defined as the cluster centroid of each cluster.
3) Obtain the final k cluster centroids and the k clusters including samples.

D. LONG SHORT TERM MEMORY NEURAL NETWORK

Long Short Term Memory (LSTM) neural network is an extension Recurrent neural network (RNN), capable of learning long term dependencies [22]. Remembering information for long periods of time is practically its default behavior, not something it struggles to learn. Unlike traditional RNN, LSTM adds three gates, forget gate, input gate and output gate. An LSTM has three of these gates to protect and control cell states.

Forget gate decides whether add or remove the historical information in the hidden layer cell. A 1 represents keep, a 0 represents remove.

Input gate decides whether the input information could be permitted add into the hidden layer cell. A 1 represents could, a 0 represents not.

Output gate decides whether transform the output value in present hidden layer cell into next. A 1 represents output, a 0 represents not.

The forward computation formulas of forget gate f_t, input gate i_t and output gate o_t are expressed as follows:

$$f_t = \sigma\left(U_f h_{t-1} + W_f x_t + b_f\right) \tag{19}$$

$$i_t = \sigma\left(U_i h_{t-1} + W_i x_t + b_i\right) \tag{20}$$

$$o_t = \sigma\left(U_o h_{t-1} + W_o x_t + b_o\right) \tag{21}$$

where σ is sigmoid activate function; U_f is the connecting weights from output of ex-hidden layer cell to present forget gate; W_f is the connecting weights from input to forget gate; b_f is the bias of forget gate; U_i is the connecting weights from output of ex-hidden layer cell to present input gate; W_i is the connecting weights from input to input gate; b_i is the bias of input gate; U_o is the connecting weights from output of ex-hidden layer cell to present output gate; W_o is the connecting weights from input to output gate; b_o is the bias of output gate. Fig. 3 is the structure of LSTM cell.

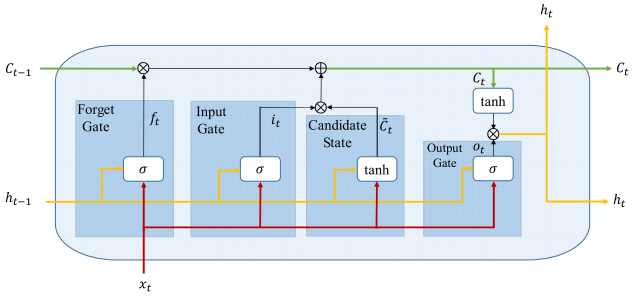

FIGURE 3. The structure of LSTM cell.

In the Fig. 3, C_{t-1} denotes ex-hidden layer cell state; $\tilde{C}_t$ denotes candidate state; C_t denotes present hidden layer cell state; tanh denotes hyperbolic tangent function; h_t is the output of present hidden cell. Their relations with forget gate, input gate and output gate are expressed by the following formulas, respectively:

$$\tilde{C}_t = \tanh\left(U_C h_{t-1} + W_C x_t + b_C\right) \tag{22}$$

$$C_t = f_t * C_{t-1} + i_t * \tilde{C}_t \tag{23}$$

$$h_t = o_t * \tanh\left(C_t\right) \tag{24}$$

E. RELIABILITY ASSESSMENT MODEL

With the increasing capacity of wind power converter, reliable and cost-effective wind energy production is more and more significant. In this part, a novel analysis and weight strategy proposed to assess reliability of wind power converter considering the confidence levels, prediction values and actual values of SCADA multistate parameters.

Selecting I state parameters S_i (i = 1,2,…, I), with whose confidence levels B_i (i = 1,2,…, I), using FP-Growth Association Rule Algorithm in Part A of Section III. Each state parameter is under the same time series with N time nodes. The nth nodes actual values of I state parameters are $S_i^{(n)} = \left\{S_1^{(n)}, S_2^{(n)}, \ldots, S_I^{(n)}\right\} \in \mathbb{R}^I, n = 1, 2, \ldots, N$. The nth nodes prediction values of I state parameters are $y_i^{(n)} = \left\{y_1^{(n)}, y_2^{(n)}, \ldots, y_I^{(n)}\right\} \in \mathbb{R}^I, n = 1, 2, \ldots, N$. Then the nth nodes reliability of wind power converter $R^{(n)}$ are expressed as follows:

$$R^{(n)} = 1 - \sqrt{\sum_{i=1}^{I}\left(\frac{S_i^{(n)} - y_i^{(n)}}{S_i^{(n)} + \sigma}\right)^2 \cdot W_i}, \quad \forall \exists R^{(n)} < 0, R^{(n)} = 0, \quad n = 1, 2, \ldots, N \tag{25}$$

$$W_i = \frac{B_i}{\sum_{j=1}^{I} B_j}, \quad i = 1, 2, \ldots, I \tag{26}$$

It should be noted that, the prediction values of multistate parameters are obtained and computed based on the normal operation data of the wind turbine. So, the prediction values is should have been the values under the normal operation. Thus, (25) denotes when the difference between actual value and prediction value of state parameter is larger, the reliability of the wind power converter is lower, conversely, the reliability is higher. Defining $R^{(n)} = 0$, if $R^{(n)} \leq 0$; σ is a tiny real number in case the denominators are zero; W_i and B_i are weight and confidence level of the ith state parameter, respectively. The higher confidence level of state parameter is, the higher weight of reliability influence is.

The reliability of wind power converter is divided into 5 levels as Fig. 4.

Level	Level 1 (Normal Operation)	Level 2 (Failure Trend)	Level 3 (Hidden Failures)	Level 4 (Frequent Failures)	Level 5 (Serious Failures)
Reliability Intervals	1-0.8	0.8-0.6	0.6-0.4	0.4-0.2	0.2-0

FIGURE 4. The reliability levels of wind power converter.

Where level 1 indicates reliability is in the range of 1-0.8, which denotes the power converter is in normal operation. Level 2 indicates reliability is in the range of 0.8-0.6, which denotes the power converter is in the failure trend, could prevent the possible faults. Level 3 indicates reliability is in the range of 0.6-0.4, which denotes there are hidden failures generate in the power converter, needed to close down and investigate. Level 4 indicates reliability is in the range of 0.6-0.4, which denotes there are failures generate frequently, should close down the wind turbine and maintain immediately. Level 5 indicates reliability is in the range of 0.2-0, which denotes the power converter is in the serious failure, the wind turbine system would shut down and alarm automatically in case harsh accidents occur.

F. MISSION PROFILE OF PROPOSED STRATEGY

In this paper, the proposed strategy for reliability assessment of wind power converter is composed of "off-line training" and "on-line matching and assessment", and considering WPT, K-means algorithm, LSTM network, analysis

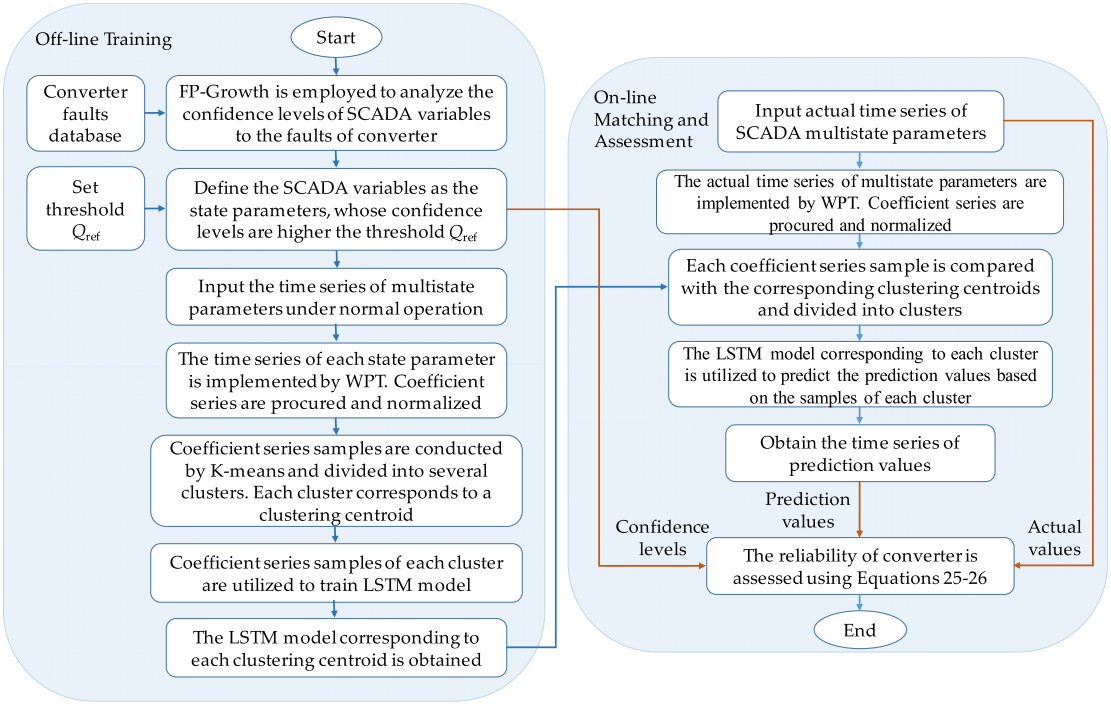

FIGURE 5. The mission profile of reliability assessment of wind power converter.

and weight. Fig. 5 is the mission profile of reliability assessment of wind power converter.

The specific steps of reliability assessment strategy are as follows.

Off-line training:

1) The FP-Growth association rule is employed to analyze the confidence levels of SCADA variables about the faults of wind power converter.

2) SCADA variables with confidence levels higher than the threshold Q_{ref} are selected as the multistate parameters to assess the reliability of wind power converter.

3) The time series of multistate parameters under normal operation of wind turbine are implemented by WPT. Coefficient series are procured and normalized.

4) Coefficient series samples are conducted by K-means and divided into several clusters. Each cluster corresponds to a clustering centroid.

5) Every cluster's LSTM prediction model is trained by taking use of coefficient series samples in corresponding cluster.

On-line matching and assessment:

1) The actual time series of multistate parameters in the same time range. are implemented by WPT. Obtained coefficient series are procured and normalized as the same as the step 3) in ''off-line training''.

2) Match the coefficient series samples closed to the clustering centroid and pointing into a cluster. The corresponding LSTM models are utilized to predict. The prediction value of a state parameter is sum of prediction value of each LSTM.

3) The reliability of wind power converter is assessed using (25)-(26) depending on confidence levels, prediction values and actual values.

IV. NUMERICAL EXAMPLES

A. DATA DESCRIPTION

To verify the validity of proposed reliability assessment strategy, a 2-MW PMSG wind turbine equipped with full scale converter is used as a case study. The most important parameters are listed in Table 1. Simultaneously, to verify the high precision of proposed prediction strategy, which is WPT, K-means and LSTM (WPT-K-LSTM), other 4 prediction strategies are utilized to compare address the same samples data, including: 1, WPT and LSTM (WPT-LSTM); 2, WPT and ELMAN (WPT-ELMAN); 3, only LSTM; 4, only ELMAN neural network (ELMAN).

TABLE 1. Parameters for a 2-MW PMSG wind turbine.

Items	Values
Rated Power	2 MW
Blade Diameter	117 m
Turbine Speed	6 to 14 rpm
Cut-in Wind Speed	3 m/s
Rated Wind Speed	9.5 m/s
Cut-off Wind Speed	22 m/s
Operation Environment Temperature	−30 ℃ to +40 ℃
Output Voltage	690 V
Output Frequency	50 Hz

In this section, firstly, the power converter faults data of several PMSG wind turbines owned by a wind farm operator

in 2018 are counted. The FP-Growth algorithm is utilized to analyze the confidence levels of 24 SCADA variables about converter faults, and 8 variables with high confidence levels are selected as SCADA multistate parameters. Then, 2000 hours' time series of SCADA multistate parameters of the wind turbine under normal operation are used as the "off-line training" samples, and 5 prediction strategies are employed for training and prediction to reflect the high precision of the proposed prediction strategy in this paper. Afterwards, 300 hours' time series of SCADA multistate parameters of the wind turbine under random operation are used as the "on-line matching and assessment" samples, which are contracted to predict by 5 prediction strategies, so as to reflect the generalization of the proposed prediction strategy. Finally, the proposed strategy is employed to address the reliability assessment of power converter. The validity of proposed strategy is verified by the log books of the wind farm.

B. ASSOCIATION ANALYSIS BETWEEN WIND TURBINE SCADA VARIABLES AND CONVERTER FAULTS

The FP-Growth association rule is employed to analyze the confidence levels of 24 SCADA variables about the faults of wind power converter. Table 2 shows the faults monitoring of several PMSG power converter systems of a wind farm operator in 2018.

TABLE 2. The examples of the wind power converter system faults.

Converter Faults	Failure Times	Failure Time (Hour)	Mean Time to Failure (Hour)
Fault Shutdown	112	3952.75	35.29
Non-Synchronous	51	1172.08	22.98
General Failure	21	433.95	20.66
IGBT Module Damaged	10	662.34	66.23
Detected Off-Grid	4	61.94	15.49
Error Shutdown	3	199.73	66.58
Not Ready	3	66.63	22.21
Error Fault Shutdown	3	269.6	89.87
Security Risk	3	473.6	157.87
Current Fault	2	4	2
Overcurrent Fault	2	383	191.5
Other Failure	2	15.2	7.6

Table 3 is the wind turbine 24 SCADA variables with their codes.

Fig. 6 presents the confidence levels of 24 SCADA variables about converter faults based on FP-Growth algorithm. Where the numbers on the abscissa axis are the codes of SCADA variables in Table 3.

It can be seen from Fig. 6 that, the confidence levels of 24 SCADA variables of wind turbine about converter faults are approximately normal distribution in the range of 0.1-0.9, which presents that some variables have a high association with converter faults, while others have a low association with converter faults. If entire 24 SCADA variables are employed as state parameters in the reliability assessment,

TABLE 3. SCADA variables of wind turbine.

Code	Variable	Code	Variable
1	Tower Sway Axial	13	Temperature of Converter Module
2	Tower Sway Transverse	14	Generator spindle speed
3	Temperature of Hub	15	Power Factor
4	Temperature of Generator Cooling Air	16	Temperature of Converter Cooling Air
5	Temperature of Bearing	17	Temperature of Battery Box 1
6	Temperature of Generator Shaft	18	Temperature of Battery Box 2
7	Hydraulic Pressure	19	Wind Speed
8	Output Phase Voltage of Converter	20	Temperature of Nacelle
9	Temperature of Main Box	21	Temperature of Top Box
10	Temperature of Converter Box	22	Line Frequency
11	Reactive Power	23	Tower Acceleration
12	Output Phase Current of Converter	24	Nacelle Position

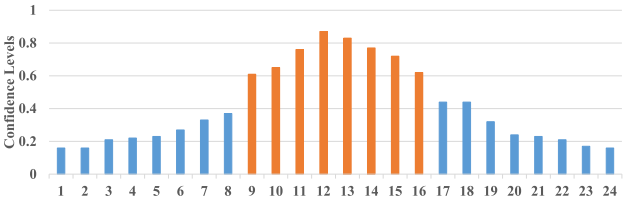

FIGURE 6. The confidence levels of 24 SCADA variables of wind turbine about converter faults.

the state parameters with low confidence levels will avianize the weight and effect of the state parameters with high confidence levels, thus reducing the effectiveness of reliability. However, if only individual high confidence variables are considered and other variables are ignored, the assessment strategy may not be sensitive to some faults of converter, thus reducing the generalization ability and accuracy of reliability assessment.

Considering the comprehensive impact of the above factors, this paper introduces threshold Q_{ref}, and selects the variables whose confidence levels are greater than threshold Q_{ref} to form the multistate parameters to assess the reliability of converter, so as to achieve a relative balance in the above-mentioned drawbacks. According to the communication with the wind farm technicians and field verification, this paper sets the threshold $Q_{\text{ref}} = 0.6$, which is also a value close to the "golden ratio" of 0.618.

Define the SCADA variables with confidence levels higher than the threshold Q_{ref} as the state parameters, which are: output current of converter, power factor, reactive power, generator spindle speed, temperature of converter module, temperature of converter box, temperature of converter cooling air and temperature of main box. In this paper, the above 8 state parameters are utilized to assess reliability of wind power converter, and their codes and confidence levels are shown in Table 4.

TABLE 4. 8 selected state parameters.

Code of State Parameter	State Parameter	Code of Confidence Level	Confidence Level Value
S_1	Output Phase Current of Converter	B_1	0.87
S_2	Temperature of Converter Module	B_2	0.83
S_3	Generator spindle speed	B_3	0.77
S_4	Reactive Power	B_4	0.76
S_5	Power Factor	B_5	0.72
S_6	Temperature of Converter Box	B_6	0.65
S_7	Temperature of Converter Cooling Air	B_7	0.62
S_8	Temperature of Main Box	B_8	0.61

C. 5 PREDICTION STRATEGIES AND ANALYSIS OF PREDICITON RESULTS

1) 5 PREDICTION STRATEGIES

5 prediction strategies are mentioned in Part A of Section IV, including:

1) WPT-K-LSTM, proposed in this paper;
2) WPT-LSTM;
3) WPT-ELMAN;
4) LSTM;
5) ELMAN.

Where ELMAN neural network is a global feed forward local recurrent proposed by Elman in 1990 [23]. It is composed of input layer, hidden layer, undertake layer and output layer. The undertake layer takes the hidden layer state of previous time together with the network input of the current time as the input of the hidden layer through connection memory, which plays a role of state feedback. Considering [short-term], the number of hidden layer neurons of ELMAN model is set to 15, and the Sigmoid activation function is employed. The mathematical expression of ELMAN neural network is as follows:

$$h_{jt}(k) = f_h[\sum_{i=1}^{m}(w_{ij}^{i}x_{it}(k) + b_i) + \sum_{j=1}^{n} w_j^r h_{jt}(k-1)] \quad (27)$$

$$y_{t+1}(k) = f_o[\sum_{j}^{m} w_j^o h_{jt}(k) + b_j] \quad (28)$$

where $h_{jt}(k)$ is the output of hidden layer neurons at t time; x_{it} is the value of time series at t time; w_{ij}^{i} is the connection weight between input layer and hidden layer; w_j^r is the connection weight between undertake layer and hidden layer; w_j^o is the connection weight between hidden layer and output layer; $y_{t+1}(k)$ is the prediction output.

2) THE ANALYSIS OF 5 STRATEGIES' "OFF-LINE TRAINING" RESULTS

In the "off-training" part, the time series of 2000 hours in the same time of 8 state parameters under the normal operation of the wind turbine are selected as samples, and above 5 prediction strategies are utilized to train them respectively, the corresponding prediction models and test results are obtained.

To compare the performance of the 5 prediction strategies and show the advantages of the proposed strategy, this paper selects 4 calculation prediction error indexes to make statistics and evaluation on the prediction results of the 5 strategies.

1) Root Mean Squared Error (RMSE):

$$RMSE = \sqrt{\frac{1}{n}\sum_{t=1}^{n}(\hat{y}_t - y_t)^2} \quad (29)$$

2) Mean Absolute Error (MAE):

$$MAE = \frac{1}{n}\sum_{t=1}^{n}|\hat{y}_t - y_t| \quad (30)$$

3) Mean Absolute Percentage Error (MAPE):

$$MAPE = \frac{100}{n}\sum_{t=1}^{n}\left|\frac{\hat{y}_t - y_t}{y_t}\right| \quad (31)$$

4) Theil Inequality Coefficient (TIC):

$$TIC = \frac{\sqrt{\frac{1}{n}\sum_{t=1}^{n}(\hat{y}_t - y_t)^2}}{\sqrt{\frac{1}{n}\sum_{t=1}^{n}\hat{y}_t^2} + \sqrt{\frac{1}{n}\sum_{t=1}^{n}y_t^2}} \quad (32)$$

where in (29)-(32), $\hat{y}_t$ is prediction value; y_t is actual value; n is the number of nodes in the time series. RMSE and MAE are related to the scale of dependent variable. They are utilized to compare different prediction results of different strategies in the same time series. The smaller the error is, the stronger the prediction ability of the strategy is. MAPE and TIC are independent of the scale of dependent variable. The values of MAPE and TIC are between 0 and 1. When they are equal to 0, it shows that the strategy is the best fitting.

Tables 5-12 are the prediction performances of 5 strategies with each state parameter, respectively.

TABLE 5. The comparison of 5 prediction methods with output phase current of power converter.

Strategy	RMSE	MAE	MAPE / %	TIC
WPT-K-LSTM	48.7619	37.6192	2.1713	0.0135
WPT-LSTM	147.5939	114.7925	6.6059	0.0415
WPT-ELMAN	173.1457	122.8435	6.6396	0.0491
LSTM	250.8485	174.8412	9.4197	0.072
ELMAN	459.3805	430.6124	23.2398	0.1439

The following conclusions can be analyzed and drawn from Tables 5-12:

1) Compared with other 4 prediction strategies, the proposed strategy WPT-K-LSTM presents the best prediction performance for 8 state parameters, the values of RMSE, MAE, MAPE and TIC are the least, and the fitting capability is the highest.

TABLE 6. The comparison of 5 prediction methods with temperature of power converter module.

Strategy	RMSE	MAE	MAPE / %	TIC
WPT-K-LSTM	0.1589	0.0693	0.0655	0.0008
WPT-LSTM	2.1711	1.8019	1.7215	0.0105
WPT-ELMAN	6.0541	5.754	5.4731	0.0299
LSTM	7.0437	6.7823	6.4604	0.0349
ELMAN	25.8012	25.7372	24.6646	0.1411

TABLE 7. The comparison of 5 prediction methods with generator spindle speed.

Strategy	RMSE	MAE	MAPE / %	TIC
WPT-K-LSTM	0.0748	0.0411	0.3565	0.0031
WPT-LSTM	0.2344	0.1907	1.6273	0.0099
WPT-ELMAN	0.4807	0.4608	3.8814	0.0206
LSTM	0.5971	0.5819	4.8975	0.0257
ELMAN	3.2368	3.2245	27.1226	0.1577

TABLE 8. The comparison of 5 prediction methods with reactive power of wind turbine.

Strategy	RMSE	MAE	MAPE / %	TIC
WPT-K-LSTM	0.4102	0.3221	25.8878	0.0816
WPT-LSTM	2.0505	1.6104	129.2377	0.5121
WPT-ELMAN	2.0568	1.7015	129.8899	0.5235
LSTM	2.8040	2.3247	189.2752	0.6965
ELMAN	2.6769	2.2257	111.5364	0.9051

TABLE 9. The comparison of 5 prediction methods with power factor.

Strategy	RMSE	MAE	MAPE / %	TIC
WPT-K-LSTM	0.00001	0.00001	0.0009	0.000004
WPT-LSTM	0.0018	0.0018	0.1817	0.0009
WPT-ELMAN	0.0135	0.0135	1.3507	0.0068
LSTM	0.024	0.024	2.4043	0.0122
ELMAN	0.0587	0.0587	5.8726	0.0303

TABLE 10. The comparison of 5 prediction methods with temperature of power converter box.

Strategy	RMSE	MAE	MAPE / %	TIC
WPT-K-LSTM	0.1538	0.0771	0.1297	0.0013
WPT-LSTM	0.3579	0.1768	0.2969	0.003
WPT-ELMAN	1.5530	1.5522	2.6158	0.0133
LSTM	1.7842	1.7833	3.0052	0.0153
ELMAN	3.758	3.7546	6.3264	0.0327

TABLE 11. The comparison of 5 prediction methods with temperature of power converter cooling air.

Strategy	RMSE	MAE	MAPE / %	TIC
WPT-K-LSTM	0.3338	0.1533	0.1858	0.0021
WPT-LSTM	0.7503	0.4149	0.5043	0.0046
WPT-ELMAN	6.6279	6.5288	8.0137	0.0425
LSTM	7.2433	7.139	8.7634	0.0467
ELMAN	20.9134	20.8885	25.7209	0.1478

2) Among the 5 prediction strategies, ELMAN has produced the worst prediction performance. When 8 state parameters are predicted by ELMAN, RMSE, MAE and MAPE

TABLE 12. The comparison of 5 prediction methods temperature of wind turbine main box.

Strategy	RMSE	MAE	MAPE / %	TIC
WPT-K-LSTM	0.0661	0.0546	0.1944	0.0012
WPT-LSTM	0.1242	0.0981	0.3488	0.0022
WPT-ELMAN	0.584	0.5725	2.0478	0.0105
LSTM	0.6928	0.6832	2.4429	0.0125
ELMAN	1.6591	1.6580	5.9187	0.0305

show the maximum values in 7 state parameters, with the largest prediction error, while TIC is the largest in 8 state parameters, with the lowest fitting capability.

3) In Table 8, the comparison of prediction performance of reactive power of wind turbine, RMSE, MAE and MAPE of ELMAN prediction results are not the maximum values. The experimental results show that the strategy has generated over-fitting phenomenon. While TIC value is the largest of the 5 prediction strategies, so the ELMAN has the lowest fitting capability.

4) The prediction performance of proposed strategy WPT-K-LSTM is higher than that of WPT-LSTM, which is mainly due to the effects of K-means clustering algorithm in the ''off-line training'' part, that is, clustering the data after WPT, which makes the reconstruction data of the test can use the corresponding LSTM model through ''on-line matching'', thus obtaining the prediction results with higher fitting capability.

5) The prediction performance of WPT-LSTM is higher than that of LSTM, and the prediction performance of WPT-ELAMN is higher than that of ELMAN, which illustrates that WPT can improve the fitting capability of prediction results before test.

6) The prediction performance of WPT-LSTM is higher than that of WPT-ELMAN, and the prediction performance of LSTM is higher than that of ELMAN, which illustrates that LSTM presents the high fitting capability for prediction results.

3) THE ANALYSIS OF 5 STRATEGIES' ''ON-LINE MATCHING AND ASSESSMENT'' RESULTS

In the ''on-line matching and assessment'' part, the time series of 300 hours in the same time of 8 state parameters under recent operation (the converter failed during this period) are selected as samples, above 5 prediction strategies are employed, and obtain the prediction results shown as Fig. 7-14. Finally, a novel analysis and weight strategy is proposed and utilized to assess reliability of wind power converter.

It can be seen from Fig. 7-14 that, most of the time, the prediction values of proposed strategy WPT-K-LSTM have generated the least error and the highest fitting capability with the actual values. At the 35^{th} hour, the actual values and prediction values of entire state parameters have a large sudden rise or fall. From the 35^{th} hour to the 86^{th} hour, compared with the actual values, the prediction results of

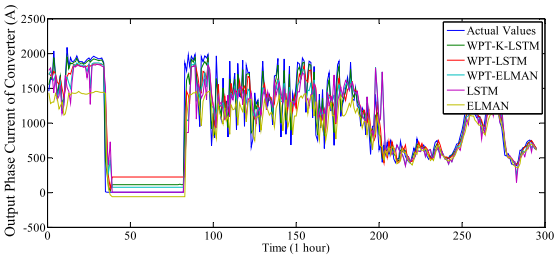

FIGURE 7. The prediction results of output phase current of power converter.

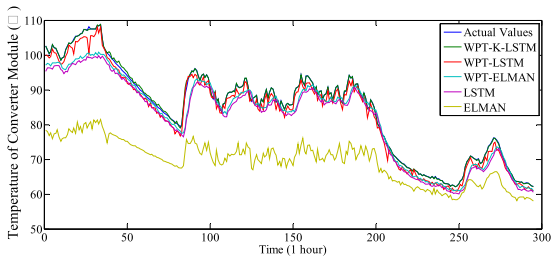

FIGURE 8. The prediction results of temperature of power converter module.

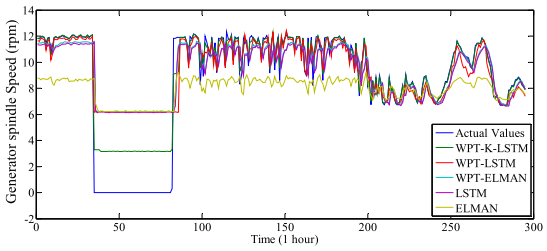

FIGURE 9. The prediction results of generator spindle speed.

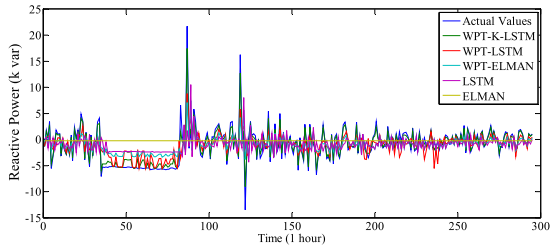

FIGURE 10. The prediction results of reactive power of wind turbine.

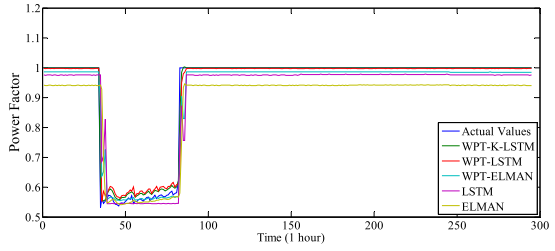

FIGURE 11. The prediction results of power factor.

all strategies show greater error and lower fitting capability. According to the inspection of maintenance records, this was caused by some fault of converter at the 35th hour, which did

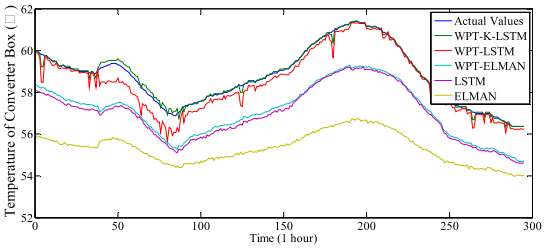

FIGURE 12. The prediction results of temperature of power converter box.

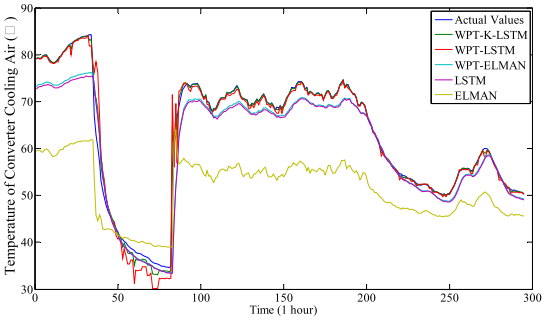

FIGURE 13. The prediction results of temperature of power converter cooling air.

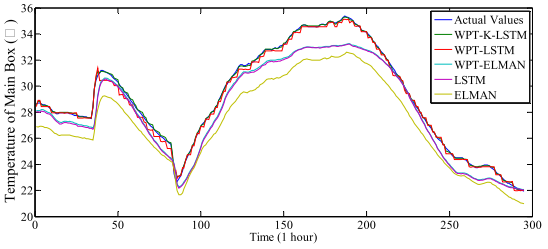

FIGURE 14. The prediction results of temperature of wind turbine main box.

not return to normal until the 86th hour. After the 87th hour, the error and fitting capability of the 5 prediction strategies to the actual values gradually returned to the original level.

D. 5 PREDICTION STRATEGIES AND ANALYSIS OF PREDICITON RESULTS

Base on the confidence levels, actual values and prediction values generated by proposed strategy WPT-K-LSTM of 300 hours, analysis and weight strategy is employed to assess reliability of wind power turbine. Figures 15 and 16 present the reliability curve of wind power converter and the active power curve of wind turbine in 300 hours, respectively.

The following conclusions can be analyzed and drawn from Fig. 15 and 16:

1) At the 35th hour, the active power of wind turbine suddenly decreased from 2000kW to about 0kW, and remained at about 0kW until the 86th hour. According to the analysis of wind power converter reliability curve and Figure 4, the wind power converter has a serious failure during this period.

2) In the following 200 hours, although the wind turbine has been in operation and the active power of the wind turbine

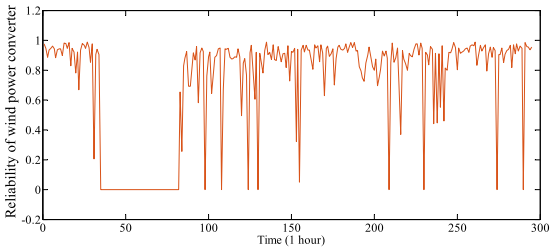

FIGURE 15. The reliability curve of wind power converter.

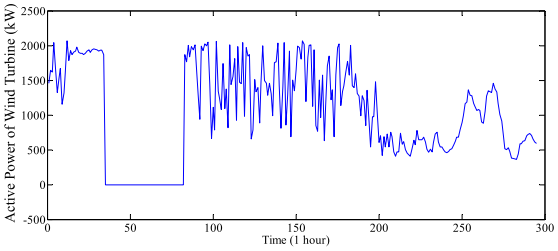

FIGURE 16. The active power curve of wind turbine.

has been kept above 400kW, the reliability of wind power converter has been reduced to 0.6-0 for many times, which indicates that the converter of the wind turbine has serious failure potential. In order to avoid serious accidents, the wind turbine should be shut down immediately and the converter should be maintained to ensure normal and stable operation of the wind power converter.

V. CONCLUSION

The main purpose of this paper is proposing a strategy containing FP-Growth, WPT, K-means, LSTM, analysis and weight to conduct the reliability assessment of PMSG wind power converter. Above all, FP-Growth algorithm is utilized to extract the high confidence level variables of wind turbine SCADA as the multistate parameters. Afterwards, the prediction model of each state parameter based on WPT, K-means algorithm and LSTM is established under normal operation of wind turbine. Conduct WPT and normalization for the ''on-line'' time series of SCADA multistate parameters. The corresponding LSTM models are employed to obtain the prediction values of each state parameters. Finally, the reliability of wind power converter is assessed by proposed strategy, which is via the analysis and weight computing of confidence level, prediction value and actual value of SCADA multistate parameters.

The numerical example results reveal that the proposed strategy has the capability to assess the reliability of the PMSG wind power converter, and are well in agreement with the field operation record.

ACKNOWLEDGMENT

J. X. Zhang would like to thank Prof. Haiyong Chen and an Engineer Wenzhong Zou for their valuable advice. The authors would like to thank all the reviewers and editors for their valuable comments and work.

REFERENCES

[1] C. Wang, L. Zhou, and Z. Li, ''Survey of switch fault diagnosis for modular multilevel converter,'' *IET Circuits, Devices Syst.*, vol. 13, no. 2, pp. 117–124, Mar. 2019.
[2] J. Zhang, H. Sun, Z. Sun, W. Dong, and Y. Dong, ''Fault diagnosis of wind turbine power converter considering wavelet transform, feature analysis, judgment and BP neural network,'' *IEEE Access*, vol. 7, pp. 179799–179809, 2019.
[3] F. Blaabjerg and K. Ma, ''Future on power electronics for wind turbine systems,'' *IEEE J. Emerg. Sel. Topics Power Electron.*, vol. 1, no. 3, pp. 139–152, Sep. 2013.
[4] B. Wu, Y. Lang, N. Zargari, and S. Kouro, *Power Conversion and Control of Wind Energy Systems*. Piscataway, NJ, USA: Wiley, 2011.
[5] Z. Yang and Y. Chai, ''A survey of fault diagnosis for onshore grid-connected converter in wind energy conversion systems,'' *Renew. Sustain. Energy Rev.*, vol. 66, pp. 345–359, Dec. 2016.
[6] T. Joseph, C. E. Ugalde-Loo, J. Liang, and P. F. Coventry, ''Asset management strategies for power electronic converters in transmission networks: Application to HVDC and FACTS devices,'' *IEEE Access*, vol. 6, pp. 21084–21102, 2018.
[7] L. Sainz, L. Monjo, J. Pedra, M. Cheah-Mane, J. Liang, and O. Gomis-Bellmunt, ''Effect of wind turbine converter control on wind power plant harmonic response and resonances,'' *IET Electr. Power Appl.*, vol. 11, no. 2, pp. 157–168, Feb. 2017.
[8] H. Zhao and L. Cheng, ''Open-circuit faults diagnosis in back-to-back converters of DF wind turbine,'' *IET Renew. Power Gener.*, vol. 11, no. 4, pp. 417–424, Mar. 2017.
[9] B. Gao, F. Yang, M. Chen, Y. Chen, W. Lai, and C. Liu, ''Thermal lifetime estimation method of IGBT module considering solder fatigue damage feedback loop,'' *Microelectron. Rel.*, vol. 82, pp. 51–61, Mar. 2018.
[10] D. Zhou, G. Zhang, and F. Blaabjerg, ''Optimal selection of power converter in DFIG wind turbine with enhanced system-level reliability,'' *IEEE Trans. Ind. Appl.*, vol. 54, no. 4, pp. 3637–3644, Jul. 2018.
[11] U.-M. Choi, F. Blaabjerg, S. Jorgensen, S. Munk-Nielsen, and B. Rannestad, ''Reliability improvement of power converters by means of condition monitoring of IGBT modules,'' *IEEE Trans. Power Electron.*, vol. 32, no. 10, pp. 7990–7997, Oct. 2017.
[12] K. Xie, Z. Jiang, and W. Li, ''Effect of wind speed on wind turbine power converter reliability,'' *IEEE Trans. Energy Convers.*, vol. 27, no. 1, pp. 96–104, Mar. 2012.
[13] D. Zhou, F. Blaabjerg, T. Franke, M. Tonnes, and M. Lau, ''Comparison of wind power converter reliability with low-speed and medium-speed permanent-magnet synchronous generators,'' *IEEE Trans. Ind. Electron.*, vol. 62, no. 10, pp. 6575–6584, Oct. 2015.
[14] Y. Hu, P. Shi, H. Li, and C. Yang, ''Health condition assessment of base-plate solder for multi-chip IGBT module in wind power converter,'' *IEEE Access*, vol. 7, pp. 72134–72142, 2019.
[15] D. Ronanki and S. S. Williamson, ''Failure prediction of submodule capacitors in modular multilevel converter by monitoring the intrinsic capacitor voltage fluctuations,'' *IEEE Trans. Ind. Electron.*, vol. 67, no. 4, pp. 2585–2594, Apr. 2020.
[16] Z. Sun and H. Sun, ''Health status assessment for wind turbine with recurrent neural networks,'' *Math. Problems Eng.*, vol. 2018, pp. 1–16, Dec. 2018.
[17] World Wind Energy Association. *Wind Power Capacity Worldwide Reaches 597 GW, 50,1 GW Added in 2018*. Accessed: Feb. 25, 2019. [Online]. Available: https://wwindea.org/blog/2019/02/25/wind-power-capacity-worldwide-reaches-600-gw-539-gw-added-in-2018/
[18] *Report on China's Wind Power Lifting Capacity in 2018 Chinese Wind Energy Association*. Accessed: Apr. 5, 2019. [Online]. Available: http://www.cwea.org.cn/news_lastest_detail.html?id=217
[19] J. Zhang, H. Sun, Z. Sun, Y. Dong, and W. Dong, ''Open-circuit fault diagnosis of wind power converter using variational mode decomposition, trend feature analysis and deep belief network,'' *Appl. Sci.*, vol. 10, no. 6, p. 2146, 2020.
[20] J. Han, J. Pei, and Y. Yin, ''Mining frequent patterns without candidate generation,'' *ACM SIGMOD Rec.*, vol. 29, no. 2, pp. 1–12, Jun. 2000.
[21] A. Laine and J. Fan, ''Texture classification by wavelet packet signatures,'' *IEEE Trans. Pattern Anal. Mach. Intell.*, vol. 15, no. 11, pp. 1186–1191, Nov. 1993.
[22] Z. Sun, S. Zhao, and J. Zhang, ''Short-term wind power forecasting on multiple scales using VMD decomposition, K-Means clustering and LSTM principal computing,'' *IEEE Access*, vol. 7, pp. 166917–166929, 2019.
[23] J. L. Elman, ''Finding structure in time,'' *Cognit. Sci.*, vol. 14, no. 2, pp. 179–211, 1990.

JINGXUAN ZHANG (Student Member, IEEE) was born in Hebei, China, in 1982. He received the B.Sc. degree in electrical automation and the M.Sc. degree in control science and engineering from the Hebei University of Technology, Tianjin, China, in 2007 and 2010, respectively, where he is currently pursuing the Ph.D. degree in control theory and control engineering. He is currently a Lecturer with the College of Electrical Engineering, North China University of Science and Technology, China. He has published seven articles on SCI and EI Journals. His research interests include reliability assessment, fault diagnosis, switched systems, and power systems. He is a PES member.

HEXU SUN (Senior Member, IEEE) received the Ph.D. degree in automation from Northeastern University, Shenyang, China, in 1993.

He has been a Professor with the School of Control Science and Engineering, Hebei University of Technology, Tianjin, China, and the School of Electrical Engineering, Hebei University of Science and Technology, Shijiazhuang, China. He has authored five books and more than 130 journal and conference papers, and holds 13 U.S. patents and five computer software copyrights. His current research interests include robotics and complex engineering systems.

Dr. Sun was a recipient of many prestigious national awards from China. He was the Director in many societies and committees in China. He is currently the invited Plenary Speaker and the General Co-Chair of many international conferences.

ZEXIAN SUN was born in Tangshan, Hebei, China, in 1991. He received the B.S. degree in automation from the North China University of Science and Technology, China, in 2013, and the Ph.D. degree in control theory and control engineering from the Hebei University of Technology, Tianjin, China. He is currently a Lecturer with the College of Electrical Engineering, North China University of Science and Technology.

WEICHAO DONG was born in Shijiazhuang, Hebei, China, in 1989. He received the B.Sc. degree in electrical Engineering and the M.Sc. degree in electrical and computing engineering from Cornell University, NY, USA, in 2012 and 2013, respectively. He is currently pursuing the Ph.D. degree in control theory and control engineering with the Hebei University of Technology, Tianjin, China.

YAN DONG (Member, IEEE) received the B.Sc. degree in electronic technology and application from China Agricultural University, China, in 1995, the M.Sc. and Ph.D. degrees in control theory and control engineering from the Hebei University of Technology, China, in 2001 and 2005, respectively. She is currently a Professor with the School of Artificial Intelligence, Hebei University of Technology, China. She has published more than 30 articles on SCI and EI Journals. Her research interests include switched systems, fault diagnosis, and power systems.

SIYUAN GONG received the Ph.D. degree in control theory and control engineering from the Hebei University of Technology, China, in 2011. He is currently working with the Hebei Construction and Investment Group Company, Ltd., after graduation. He has authored one book and eight journal and conference papers and holds six computer software copyrights. His current research interests include fault diagnosis and data mining.